Overlimiting mass transfer through cation-exchange membranes modified by Nafion film and carbon nanotubes

E.D. Belashova, N.A. Melnik, N.D. Pismenskaya, K.A. Shevtsova, A.V. Nebavsky, K.A. Lebedev, V.V. Nikonenko *

Membrane Institute, Kuban State University, 149 Stavropolskaya St., 350040 Krasnodar, Russia

A B S T R A C T

Eight cation-exchange membranes different in the surface morphology and the degree of hydrophobicity were studied by contact angle, voltammetry and mass transfer rate measurements. One series of membranes was prepared starting from heterogeneous MK-40 membranes, and another, from homogeneous Nafion[TM] 117 membranes. Coating a membrane with a thin film of Nafion resulted in increasing surface hydrophobicity, while the doping of the Nafion surface film with carbon nanotubes (CNT) led to an unexpected decrease in hydrophobicity. It was found however that after 100 h operation of a Nafion[TM] 117 membrane coated with a Nafion film doped with CNT, the contact angle increased from 51 to 81°. This increase in the surface hydrophobicity was accompanied by a significant rise in overlimiting transfer rate, more than 1.5 times, under the same voltage. High correlation between the overlimiting mass transfer rate and the degree of hydrophobicity was observed also in all studied cases: more hydrophobic surface leads to a higher mass transfer rate. The effect is explained by increasing electroconvection occurring as electroosmosis of the second kind: the slip of water over a hydrophobic surface enhances the tangential velocity of electroconvective vortex having its maximum at a distance of several hundreds of nm from the surface.

© 2011 Elsevier Ltd. All rights reserved.

1. Introduction

It is known that the main mechanism of overlimiting transfer of salt ions in ion-exchange membrane systems at diluted solutions is electroconvection [1–5]. Electroconvection arises due to the action of an externally applied electric field on the electric space charge in the boundary depleted solution [6–10]. Dukhin and Mishchuk [7,8,11] first studied this current-induced phenomenon and distinguished its two principal mechanisms. At low current densities electroconvection occurs as electro-osmosis of the first kind, which is the fluid slip caused by the action of the electric field upon the diffuse part of the electric double layer (EDL). The latter always exists at the membrane/solution interface and remains quasiequilibrium under low currents. The electro-osmosis of the second kind (named also induced-charge electroosmosis [12,13]) is similar to that of the first one with the difference that the electric field acts upon the extended nonequilibrium space charge region (SCR) induced by the same electric field. The extended SCR may attend the

thickness of the order of $1\,\mu m$ [14] at high voltages, about 8 V per a cell pair (which is a repeating unit of an electrodialysis stack involving one anion- and one cation-exchange membranes with one desalination and one concentration compartments). The electroosmotic slip may produce microvortices, which contribute to the delivery of fresh solution onto the membrane surface. Otherwise, this slip may be used to realise directed motion of fluid as in micropumps. Generally, it is a means to transform electric energy into mechanical energy of moving fluid.

Electroconvection is an important facility of enhancing electrodialysis of dilute electrolyte solutions [1,11,15]. This phenomenon is also crucial in electrophoresis [16], electrodeposition [17], in electrokinetic micro- and nanofluidic devices [18–20] such as micropumps [21–23] and other applications [24].

Electroconvection is affected by a number of factors. The most important is the ratio of the flowing current density to the limiting current density (this ratio is a function of the applied voltage). Rubinstein and Zaltzman [6] have theoretically found three different modes of electroconvection: a stable mode where the electroconvective vortices do not vary with time, after a number of decaying oscillations; a mode of periodic oscillations of vortices; and a mode where the oscillations become chaotic. These three modes of vortex oscillations manifest themselves through corresponding oscillations of current density under a constant voltage, or the oscillations of voltage under a constant current. In the

* Corresponding author at: Physical Chemistry Department, Kuban State University, 149 Stavropolskaya Str., 350040 Krasnodar, Russia. Tel.: +7 861 2199 573; fax: +7 861 2199 517.
  E-mail addresses: nikon@chem.kubsu.ru, v_nikonenko@mail.ru (V.V. Nikonenko).

latter case, three different types of voltage oscillations predicted by Rubinstein and Zaltzman [6] were experimentally observed by Belova et al. [4].

Furthermore, electrical and geometrical surface inhomogeneity essentially influence electroconvection [6,3]. The theory [6,25] predicts hastening the onset of overlimiting transfer because of inhomogeneous distribution of the space charge density on the membrane surface. This follows from the general condition of the electroconvection occurrence: for the appearance of electroconvection, it is necessary that the curl of the volume force, which is the product of the electric field and the space charge density, should be non-zero [26]. Note that in the case of flat homogeneous surface, a non-zero curl arises due to instability of quiescent electric conduction [6]. It arises also because the thickness of the diffusion boundary layer (DBL) is not uniformly distributed along the membrane. In the case of relief/profiled/undulated membrane surface, a tangential electric field component occurs in addition to the space charge inhomogeneity, and its application to the SCR near a sloping surface brings liquid in motion more effectively than it takes place at a flat surface [27,2]. In the case of waved surface, the voltage threshold for the appearance of the vortex flow should be noticeably less than that for a flat membrane [8], or even absent [6]; a 10% distortion of the flat membrane surface results in a 30% increase in the current resulting from partial destruction of the DBL [6].

The rate of electroconvection depends as well on the Stokes radius of counterions forming the SCR. (The Stokes radius of an ion is the radius of a hard sphere, close to that of the hydrated ion, which exhibits the same hydrodynamic property as the ion). Indeed, the more this radius, the more effective the liquid is involved in motion. Choi et al. [28] have compared the I–V curves measured in solutions of different electrolytes and found that the relative increment in overlimiting current increases with the Stokes radius. The case of H^+ and OH^- ions is particular, as they have a rather small Stokes' radius due to strong contribution of the Grotthus transport mechanism of these ions: they carry the charge by "tunnelling" from one water molecule to another without bringing liquid volume into motion. As a result, water splitting occurring at membrane interface under high voltages suppresses the electroconvection, as H^+ (OH^-) ions invade the SCR and replace salt counterions having relatively large Stokes' radius [4]. Another consequence of this effect is that the increment of the overlimiting current, when using NaCl solutions, is relatively higher in the case of cation-exchange membranes in comparison with the anion-exchange ones [29]. The reason is that the Stokes radius of Cl^- is less than that of Na^+ [30]. Moreover, water splitting is as usual more intensive at anion-exchange membranes [31,32,28], having ion-exchange groups catalytically more active towards water splitting [33,34].

We have recently found [5] that the overlimiting mass transfer rate through an ion-exchange membrane is strongly affected by the degree of its surface hydrophobicity. For several cation-exchange membranes studied, different in surface morphology, the overlimiting mass transfer increased in the same range as the water contact angle characterizing surface hydrophobicity.

This paper is aimed at better understanding of the relationship between the ion-exchange membrane surface properties, the degree of its hydrophobicity in particular, and the overlimiting mass transfer in conditions where the enhancement of the mass transfer is mostly controlled by electroconvection.

Several ion-exchange membranes with different morphologies and different degrees of the surface hydrophobicity are studied. The idea is to modify the surface of a heterogeneous cation-exchange membrane in several ways, in order to decrease its hydrophobicity (by mechanical removal of surface hydrophobic layer) or to increase it (by coating the surface with a Nafion film containing or not carbon materials of a high hydrophobicity), and to see how these modifications affect the overlimiting transfer.

Note that surface modification of ion-exchange membranes is a cost effective way to prepare new membranes with desired properties, in particular, effective for overlimiting transfer intensification via increasing electroconvection. This practical aspect is important for electrodialysis and for other applications, which use overlimiting transfer modes.

2. Experimental

2.1. Membranes

Several cation-exchange membranes were studied prepared on the basis of a heterogeneous Russian cation-exchange membrane MK-40 and a homogeneous perfluorinated sulfonated membrane Nafion™ 117. The MK-40 membrane is produced from powdered cation exchange resin KU-2 (a sulfonated copolymer of styrene and divinylbenzene) in the sodium form, making 65 vol.% [35], and low-pressure polyethylene. We have studied samples of MK-40 taken from two different lots. They differed in the fraction of the surface available for the ion transfer (the other part of the surface is coated by the binder, polyethylene). For the first lot (the samples are denoted as MK-40), the fraction of the ion-conducting area is (0.22 ± 0.03), for the second one (denoted as MK-40′), it is 0.30 ± 0.05.

The surface of MK-40 is modified in three ways:

- the first sample is the MK-40 membrane subjected to a special roughing (removal of a surface layer using an abrasive) (MK-40*);
- the second sample is a roughed MK-40 membrane coated with a thin layer of Nafion™ (of 5 and 20 μm thickness) (MK-40*/Nf$_5$ and MK-40*/Nf$_{20}$);
- the third sample is a roughed MK-40 membrane coated with a thin (of about 20 μm thickness) layer of Nafion™ doped with a carbon material, a mixture of carbon nanotubes and amorphous carbon (MK-40*/Nf + CM). The liquid Nafion™ contained about 5% of ultrasound-dispersed CM.

For comparing the properties of composite membranes prepared on the basis of MK-40, a Nafion™ 117 (Nafion) and two its modifications are studied:

- an original Nafion™ 117 membrane coated with a Nafion™ film (Nafion/Nf);
- a Nafion™ 117 membrane coated with a Nafion™ film containing multiwall ultrasound-dispersed carbon nanotubes (Nafion/Nf + CNT).

The main properties of MK-40 and Nafion™ 117 membranes are shown in Table 1.

2.2. Measurements

Visualizations of membrane surface and cross-sections were performed using scanning electron microscopy (SEM). We used a scanning electron microscope JSM-7500 F.

The contact angles on the membrane surface, in the sodium form, were measured by the sessile drop method. This technique [36] differs from the traditional ones [37,38] by that the membrane is in swollen state, pre-equilibrated with a solution (0.02 mol dm^{-3} NaCl). A drop of a 0.02 mol dm^{-3} NaCl solution of approximately 7 μL in volume was applied from a height of 0.7 cm on the membrane surface. The membrane was removed from the equilibration solution just before the measurements. It is placed in a closed optically transparent box on a filter paper, which is in contact with the same 0.02 mol dm^{-3} solution of NaCl. The residual solution film on

Table 1
Characteristics of membranes MK-40 and Nafion™ 117.

Membrane	Binder	Matrix	Exchange capacity (meq cm^{-3})[a]	Thickness (μm)[a]	Water content (g$_{H_2O}$ g^{-1})[a]
MK-40	Polyethylene	Sulfonated polystyrene with divinylbenzene	1.74	410	0.29
Nafion™ 117	–	Sulfonated tetrafluoroethylene	0.76	220	0.15–0.20

[a] For swollen membrane in the Na$^+$ form.

the membrane side faced to the liquid dozer is quickly removed. The images obtained with a digital video camera are processed using computer program ImageJ to improve the contrast of the contours of the drop. 20 s after the application of a drop, the inflow wetting angle on the membrane surface is found using the tangent method. The experiment is repeated no less than 10 times. The drop is placed onto various parts of the membrane surface; then the average value of the contact angle and the inaccuracy is calculated. The standard deviation of determining the angle is 3–4°.

This method allows us to keep the membrane in conditions close to thermodynamic equilibrium with a solution. Moreover, these conditions are similar to the real state of membrane in electrodialysis.

The total I–V and mass transfer characteristics of the membrane were measured in a 0.02 mol dm^{-3} NaCl solution by using the set-up and the method described in detail in [4,29].

A feature of the used electrochemical flow cell (Fig. 1) is special comb-like input/output hydraulic arrangements. They provide a laminar hydrodynamic regime in the intermembrane space containing no filler. The mass transport in the desalting channel of this cell is well described by the convection-diffusion theory [39]. The theory allows calculation of the value of limiting current, which can be achieved in the absence of secondary effects of concentration polarization (such as electroconvection, gravitational convection, and water splitting). In this case the Lévêque equation in the one-term approximation form for calculating the limiting current density averaged over the desalination path of length L can be used [40]:

$$j_{\lim}^{theor} = 1.47 \frac{FDC_0}{h(T_i - t_i)} \left(\frac{h^2 V}{LD} \right)^{1/3}, \tag{1}$$

where F is the Faraday constant, D and C_0 are the diffusion coefficient and the inlet concentration of electrolyte (NaCl); h is the intermembrane spacing; T_i and t_i are the effective [39] (or integral [5]) transport number of the counterion i in the membrane and its transport number in solution; V is the average linear velocity of solution flow between the membranes. T_i is defined as the current fraction carried by ion i through the interface or the membrane in steady state under all forces applied [5]. Eq. (1) may be applied to any type of electrolyte (the inlet concentration should be in eq.dm^{-3}); it is satisfied if the length L is sufficiently short: $L \leq 0.02\, Vh^2/D$ [39].

The calculation of the limiting current density with Eq. (1) for the inlet concentration 0.02 mol dm^{-3} NaCl and the described above experimental conditions gives $j_{\lim}^{theor} = 2.0$ mA cm^{-2} in all cases except that represented in Fig. 6b for which $j_{\lim}^{theor} = 2.5$ mA cm^{-2}.

To measure the concentration dependence of the mass transfer coefficient, the desalination process is realized in quasi-steady-state circulation mode when the desalting stream passes through a tank (Fig. 1) by keeping a slow (less than 1% per minute) decrease in the electrolyte concentration of the solution in the tank [41,42] (Fig. 1). The temperature and the pH of the solution in the tank are maintained constant. Before the experiment, the tank, the cell compartments and the hoses are filled with a 0.03 mol dm^{-3} NaCl solution. The experiment is performed under a constant $\Delta\varphi$ between the Luggin capillaries (shown in Fig. 1) at 25 ± 0.5 °C. The distance between the tip of a Luggin capillary and the membrane

is about 1 mm. The electric current and the specific conductivity of the solution (converted then into the NaCl concentration) in the tank are measured as functions of time.

The NaCl concentration in the tank varies with time due to ion transfer through IEMs in the ED cell, and due to adding of alkaline (or acid) solution into the tank in order to maintain pH = 7. The description of material balance in the tank leads to the equation:

$$k_1 = \frac{j_1}{FC} = -\frac{V_{sol}}{SC}\frac{dC}{dt} + \frac{c_T W_T}{SC}, \tag{2}$$

where j_1 is the partial current density of counterion (1) through the membrane under study; C, the electrolyte (NaCl) concentration in the tank; k_1 (defined as j_1/FC), the mass transfer coefficient, characterizing the salt counterion transfer rate through the membrane under study; V_{sol}, the volume of solution in the desalting stream (including its volume in the tank, in the desalting compartment of the cell and in the hoses); W_T and c_T, the volume rate and the concentration of the solution (NaOH or HCl) added into the tank to maintain constant its pH value; S, the membrane active surface. In our experiments we recorded electrolyte concentration of the solution in the tank (by measuring its electrical conductivity) and the volume of the added (NaOH or HCl) solution every 60 s; the value of V_{sol} was calculated taking into account the amount of the added solution. The full duration of the experiment was 6–8 h; decrease of concentration was less then 0.5% in min. The value of dC/dt was found by differentiating the curve $C(t)$. Then k was calculated according to the right-hand side of Eq. (2). The confidence interval in determining k was ±5%.

Eq. (2) assumes that there is no co-ion flux through both membranes forming the desalination compartment. This equation is applied if the mass transfer coefficient is determined for the salt counterion passing through the membrane, which generates less H$^+$ and OH$^-$ ions than the other one forming the desalination compartment. It is the case of Na$^+$ transfer through the MK-40 membrane, if it is used together with a MA-40 M anion-exchange membrane characterized by reduced function of the generation of H$^+$/OH$^-$ ions [43]. In this case, the pH of inlet and outlet solutions were very close, and only when the inlet solution was quite dilute (<0.01 mol dm^{-3} NaCl), a small amount of NaOH was added in the tank to compensate the excess of H$^+$ ions produced at the MA-40M membrane.

In all cases except that presented in Fig. 6b, the polarized by electric current area of the membrane was $S = 2$ cm × 2 cm, the intermembrane distance $h = 6$ mm; the average linear velocity of solution flow between the membranes $V = 0.4$ cm s^{-1}. In the case of Fig. 6b, S was the same while $h = 5$ mm and $V = 0.6$ cm s^{-1}. The membranes in our experiments were arranged horizontally. The depleted (lighter) diffusion layer was at the bottom of the membrane under study that excluded gravitational convection near its surface [44].

3. Results and discussion

3.1. Surface morphology

The surface of commercially produced MK-40 membrane includes two kinds of regions. The conducting regions are formed
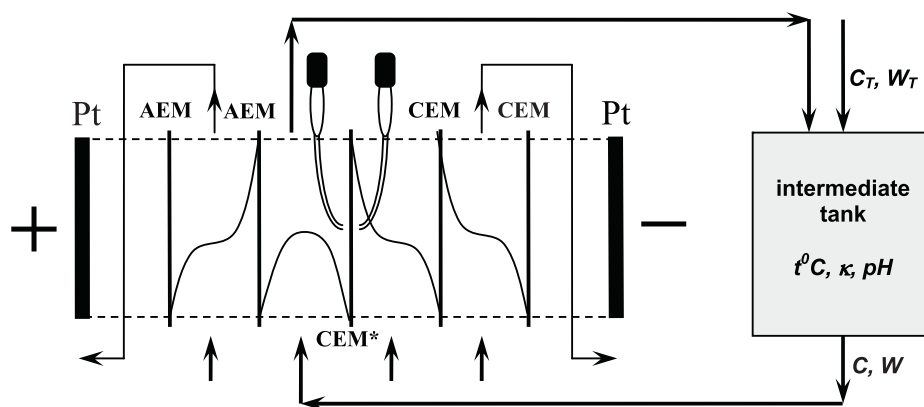
Fig. 1. Scheme of the electrochemical flow cell with anion-exchange (AEM) and cation-exchange (CEM) membranes (an asterisk denotes the membrane under study) used for voltamperometry and mass transfer measurements. The curves schematically show concentration profiles in the cell compartments.

by ion-exchange resin particles rising above the non-conducting regions, which are polyethylene used as binding material for reinforcing the membrane. The average size of conducting particles is about 30 μm, they are spaced by 100 μm (Fig. 2 a). After roughing, a part of the polyethylene covering the surface is removed, hence the fraction of the area occupied by the resin particles on the surface increases.

The hot pressing method of fabrication of MK-40 membranes results in higher polyethylene content in the surface layer. According to conditions of pressing, the surface fractions occupied by the resin particles or polyethylene may vary. As we mentioned in Section 2, in the case of MK-40 (the first lot) about 78% of

the surface is occupied by polyethylene [45], while in the case of MK-40′ it is about 70%. This non-uniform distribution of polyethylene is well seen in Fig. 2c. Mechanical treatment of the surface of MK-40 removes the surface layer rich in polyethylene and results in increasing surface fraction of conducting hydrophilic regions (Fig. 3).

Coating the surface of the MK-40* membrane with a Nafion™ film homogenizes the near-surface layer (Fig. 4). Introduction of carbon material (which is a mixture of carbon particles of the size 0.5–5 μm) into this layer leads to a specific surface heterogeneity: carbon material is unevenly distributed over of the Nafion surface, forming "islands" of about 10–100 μm in diameter, which occupy
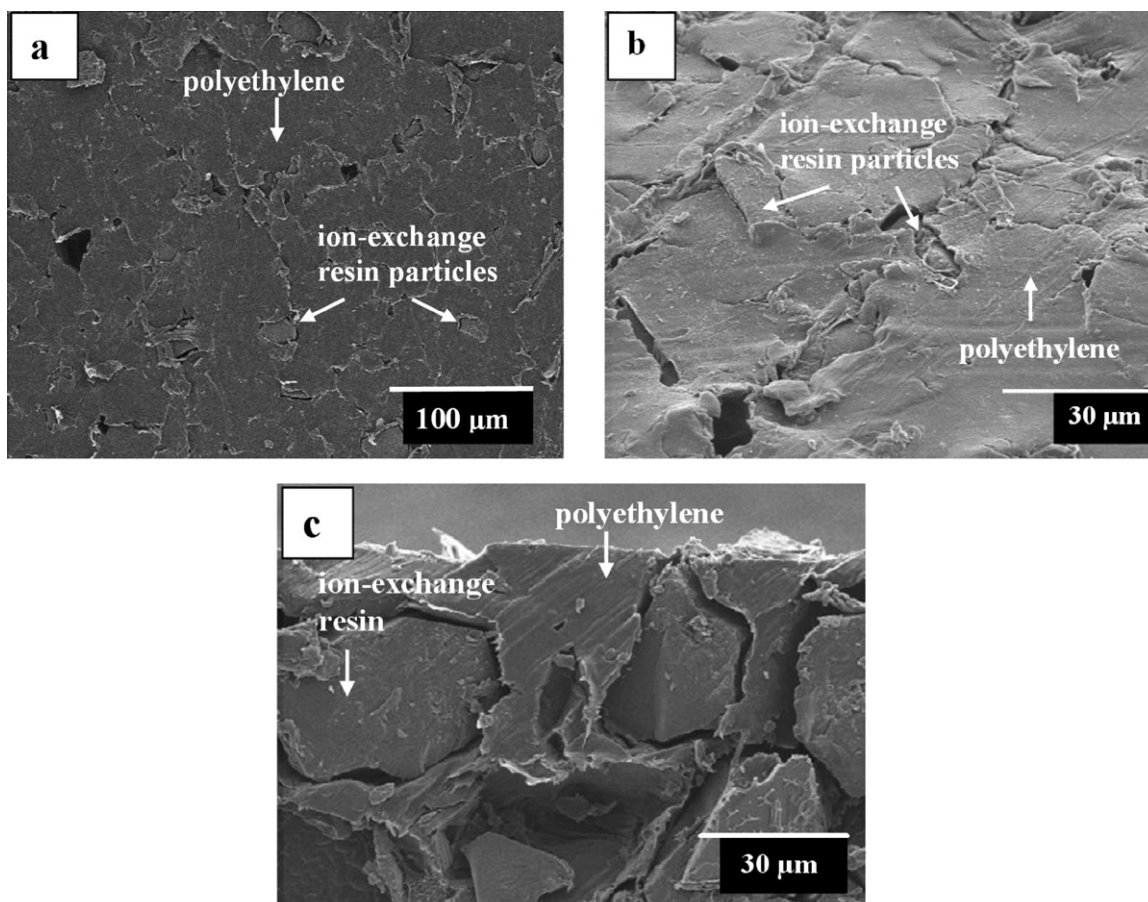

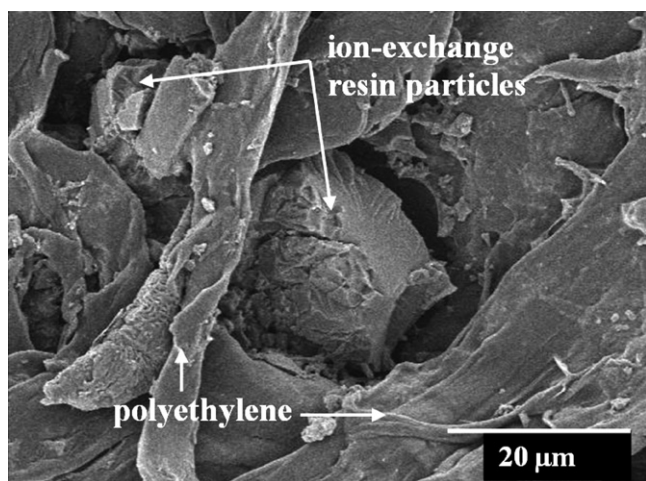**Fig. 2.** SEM image of the surface (a, b) and the cross section (c) of a MK-40 membrane.

Fig. 3. SEM image of the surface of a MK-40* membrane.

Table 2
Water contact angles on the surface of the MK-40-based membranes.

Membrane	Contact angles
MK-40	55
MK-40′	39
MK-40*	32
MK-40*/Nf	64
MK-40*/Nf + CM	39

near 15% of the surface. The value was found by using Corel Photo-Paint after contrasting a SEM microphotography [45].

Nafion/Nf + CNT membranes have a similar morphology. CNT, as well as carbon material in the case of MK-40*/Nf + CM, from conglomerates of the size of 10–100 μm covering about 15% of the surface (Fig. 5a). The surface of a CNT cluster is undulated (Fig. 5b). The clusters of CNT are separated from the solution by a very thin "wall" of Nafion polymer. The presence of this wall can be observed in Fig. 5c: a part of nanotubes is relatively well seen, while the other part is as in a fog because they are separated from the surface by a layer (wall) of Nafion material. Each nanotube is as well separated from another one, there is Nafion material between them.

3.2. Contact angle

The contact angles found for the MK-40-based membranes are shown in Table 2. As expected, the mechanical treatment of the surface of MK-40 resulted in a decrease of hydrophobicity. The MK-40′ membrane having higher fraction of hydrophilic ion-conducting regions is characterised by lower contact angle in comparison with the MK-40 one. The application of Nafion film on the roughened MK-40 strongly enhanced the surface hydrophobicity. And the introduction of highly hydrophobic carbon material into the surface film reduced the surface hydrophobicity, against the expectations.

The decrease in hydrophobicity resulted from the mechanical treatment of the surface is explained, as mentioned above, by the fact that a near-surface layer rich in hydrophobic

polyethylene is removed. The coating of MK-40* membrane with a Nafion film makes its surface more hydrophobic due to the perfluorinated matrix of Nafion. The contact angle of Teflon having the same chemical structure as the matrix of Nafion is 115° that is noticeably higher than that of polystyrene (86°) making the matrix in KU-2 cation-exchange resin, the main component of MK-40. Besides, the polyethylene, the second component of MK-40, is characterized by the contact angle equal to 92°. The hydrophobic/hydrophilic balance of an ion-exchange membrane surface is determined not only by its matrix polymer material generally highly hydrophobic, but also by the fixed ions, which attract water molecules. The morphology of such membranes (or the resins constituting the main part of them) may be presented as a system of hydrophilic conducting channels confined within a hydrophobic polymer phase [46]. The exchange capacity and water content of MK-40 are higher than respective parameters of Nafion (Table 1) that contributes into higher hydrophilicity of MK-40 and MK-40*.

These differences in properties explain relatively low hydrophobicity of MK-40 and high hydrophobicity of Nafion (Table 2). The contact angle of MK-40*/Nafion film is lower than that of Nafion membrane. It is due to the fact that the Nafion film is thin (20 μm, measured as the difference in the thickness of the unmodified and modified membranes with a digital micrometer), and a few number of resin particles of MK-40 rise over the film surface (Fig. 4a).

The relatively low value of the contact angle on the MK-40*/Nf + CM is explained by a very thin wall of Nafion separating carbon material from the solution. This film of Nafion appears as the particles of carbon material are dispersed within the liquid Nafion applied for making a layer on a membrane used as a support. Apparently, a reorientation of polymer chains within this Nafion wall takes place [37]: due to hydrophobic/hydrophobic interactions, the hydrophobic parts of the film (backbone chains) are attracted towards the CNT, while the hydrophilic parts (side chains with fixed charged groups) are oriented towards the solution. As a result, the hydrophobicity of a membrane coated with a Nafion film doped with carbon material should be lower than that of bulk commercial Nafion. To verify this hypothesis, we have prepared a composite membrane taking an commercial Nafion[TM] 117 membrane as a
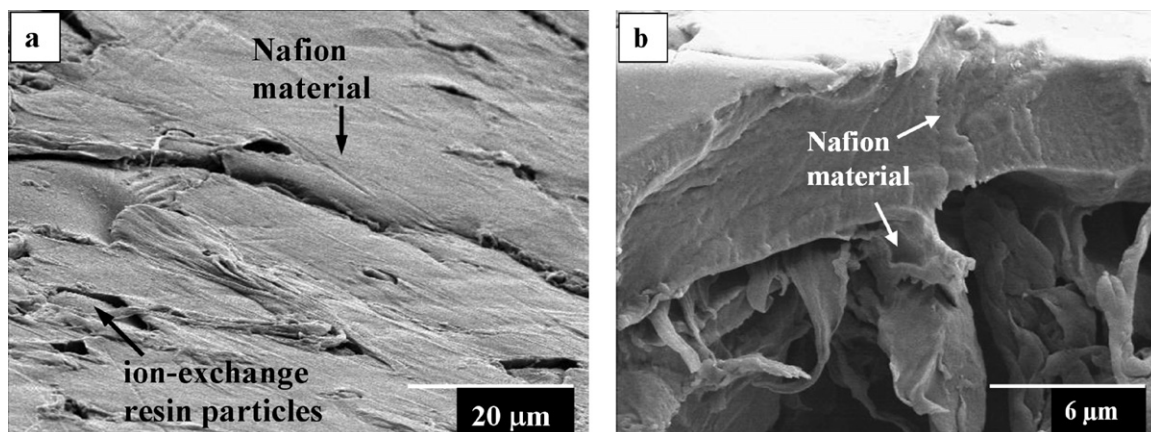

Fig. 4. SEM image of the surface (a) and the cross section (b) of a MK-40*/Nf membrane.

Table 3
Water contact angles on the surface of "fresh" and operated under electric current Nafion-based membranes.

Membrane	Wetting contact angle of "fresh" membrane	Wetting contact angle of used membrane
Nafion™ 117	66	66
Nafion/Nf	65	61
Nafion/Nf + CNT	51	81

support, and coating it with a Nafion™ film containing multiwall CNT. A thin polymer film (a "wall" of the order of 100 nm) separating CNT from the solution is well seen in the microphotography (Fig. 5c).

The contact angle on the surface of Nafion/Nf + CNT membrane was found to be not very far from that on the MK-40*/Nf + CM membrane (Table 2). Apparently the ion-exchange resin particles projected over the Nafion film on the surface of MK-40*/Nf + CM make this membrane more hydrophilic in comparison with Nafion/Nf + CNT membrane. Note that the chain reorientation should not occur if a Nafion membrane is coated with a Nafion film without CNT. Indeed, as Table 3 shows, in this case the contact angle is close to that on the supporting Nafion membrane.

3.3. Voltammetry

Current–voltage characteristics of MK-40-based membranes are presented in Fig. 6a and b. Comparison of the data presented in these figures and those in Table 2 shows that there is a strong correlation between the rate of overlimiting transfer and the degree of surface hydrophobicity of studied membranes: generally the more hydrophobic the surface, the more intensive is the overlimiting transfer.

It should be noted that the partial current of hydrogen ion produced in water splitting is very low (not exceeding 10%, within the experimental error) for all membrane samples, in comparison with the total current. Therefore, the observed increase in the total current over its limiting value cannot be attributed to the contribution of H^+ ions generated at the surface during water splitting. In other words, the main cause of the strong increase in the overlimiting current (resulted from the membrane surface modification) is the enhancement of the Na^+ ion transfer through the membrane.

The limiting current density calculated by Eq. (1) is equal to 2.0 mA cm^{-2} for the conditions of Fig. 6a and 2.5 mA cm^{-2} for those of Fig. 6b (see Section 3). These theoretical values are close to the corresponding experimental limiting current densities (found by the intersection of tangents drawn to the initial and "plateau" regions of the I–V curve) in the case of MK-40, MK-40′, MK-40* and MK-40*/Nf$_{20}$ + CM membranes. However, in the case of MK-40*/Nf$_{20}$, MK-40′/Nf$_5$, MK-40′/Nf$_{20}$ and Nafion membranes the experimental limiting current density is higher.

3.4. Role of surface hydrophobicity

As we mentioned in Section 1, surface electric and topological inhomogeneities enhance electroconvection. However, it seems that the factor of hydrophobicity is more important than that of surface inhomogeneity: MK-40, MK-40* and MK-40′ are heterogeneous, their surface is electrically inhomogeneous. However, the limiting and overlimiting mass transfer through these membranes
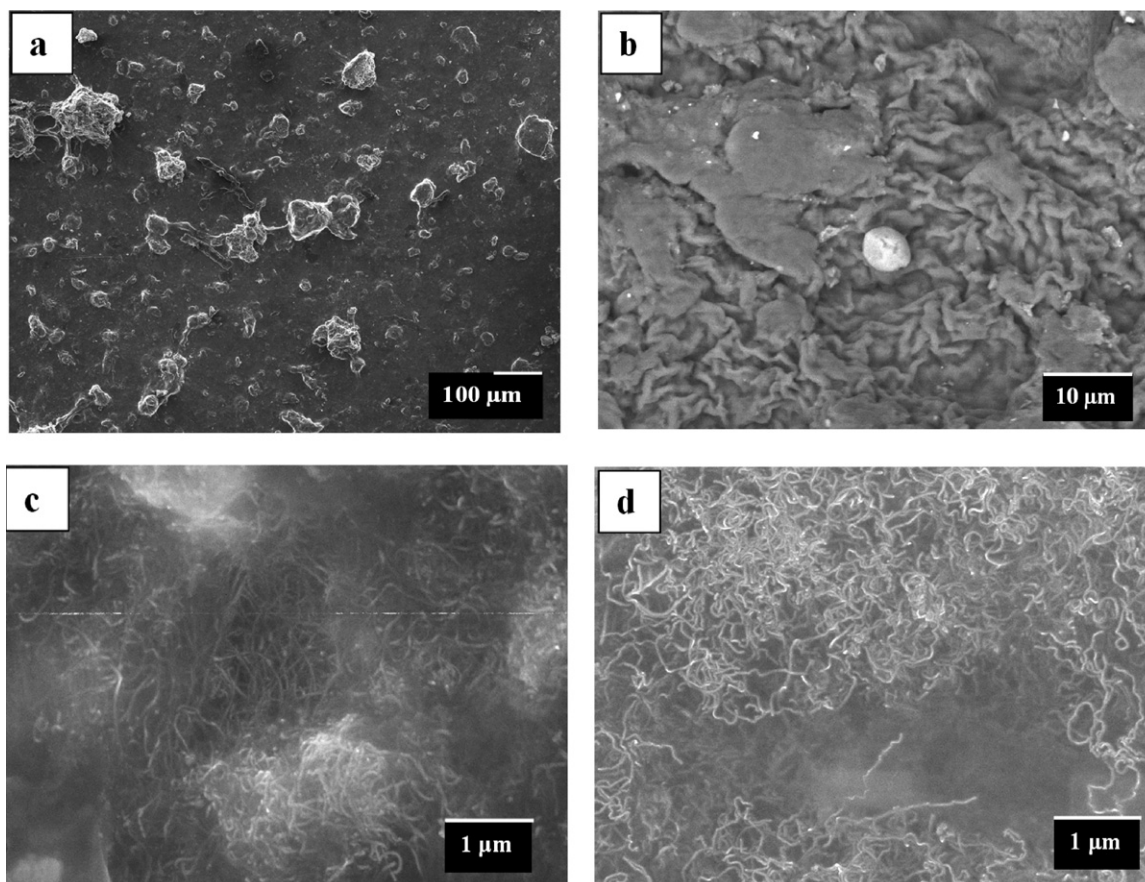

Fig. 5. SEM image of a Nafion/Nf + CNT membrane; (a)–(c) a "fresh" membrane non-treated under current; (d) a membrane treated under an overlimiting current $j = 1.5 j_{lim}^{theor}$ for 100 h.
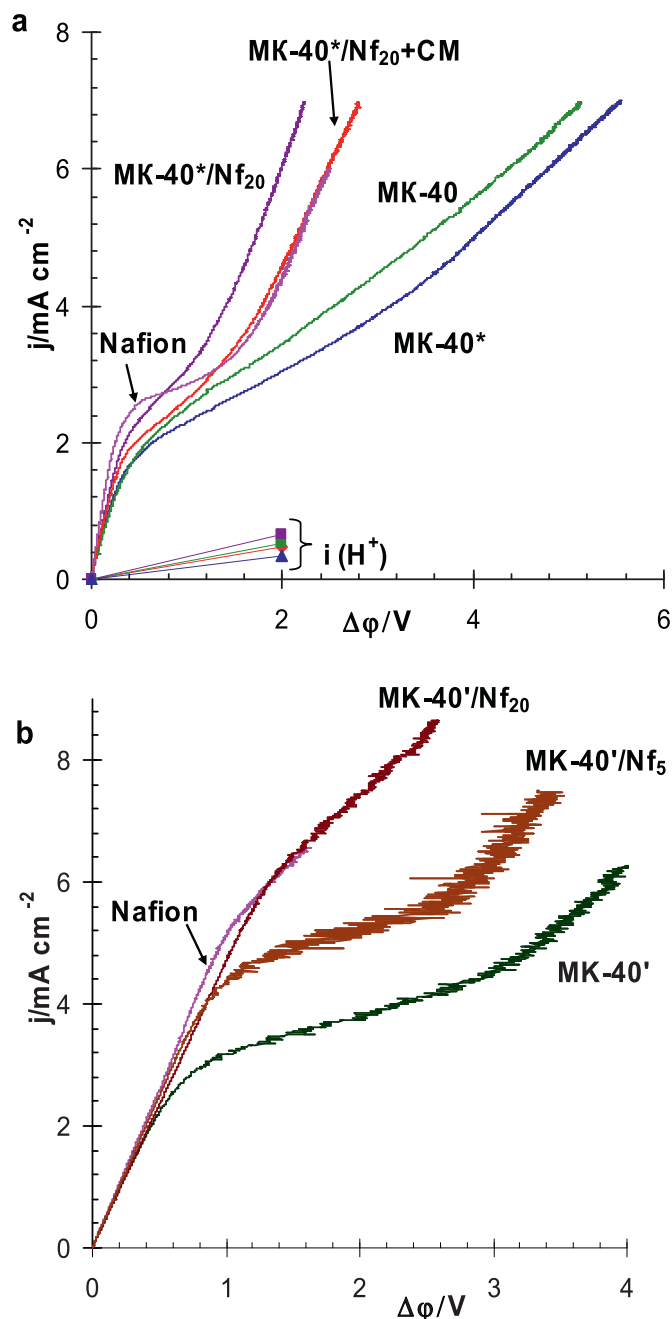
a

b

Fig. 6. Total current density and partial current density of ions H^{+} [i(H^{+}) in (a)] through MK-40 and its modifications (a) and MK-40′ and its modifications (b). (a) $h = 6$ mm, $V = 0.4$ cm s^{-1}, $j_{lim}^{theor} = 2.0$ mA cm^{-2}; "fresh" membranes soon after preparation; (b) $h = 5$ mm, $V = 0.6$ cm s^{-1}, $j_{lim}^{theor} = 2.5$ mA cm^{-2}; membranes after about 100 h of operation under an intensive current. The data for Nafion^{TM} 117 membranes are shown for comparison. The thickness of the Nafion layer on MK-40′ is 5 (MK-40′/Nf$_5$) or 20 (MK-40′/Nf$_{20}$) μm.

is lower than that in the case of homogeneous, but more hydrophobic MK-40*/Nf$_{20}$, MK-40*/Nf$_{20}$ + CM (Fig. 6a) as well as MK-40′/Nf$_5$ and MK-40′/Nf$_{20}$ (Fig. 6b) membranes. The thicker the film of Nafion coating a MK-40 membrane, the higher the hydrophobicity of the surface. It is explained by the fact that when the thickness of Nafion film is small, a part of highly hydrophilic cation-exchange resin particles rise over the surface. In the case of a sufficiently thick Nafion film (about 20 micrometers or more), the degree of hydrophobicity of MK-40/Nf and Nafion-117 membranes becomes almost equal. As a result, the I–V curve of MK-40′/Nf membrane tends

to that of Nafion^{TM} 117 with increasing the Nafion film thickness (Fig. 6b).

On the other hand, the overlimiting mass transfer through the MK-40* membrane obtained by roughing an MK-40 membrane, is lower than that through the MK-40 (Fig. 6a). Apparently, the main cause is the decrease in the surface hydrophobicity (Table 2): this decrease is due to the fact that a part of polyethylene coating the surface of MK-40 is removed, and the fraction of highly hydrophilic cation-exchange resin particle on the surface increases (Fig. 3).

It is of interest that the overlimiting mass transfer through the MK-40* membrane is lower despite the fact that the fraction of conducting surface regions for this membrane is higher in comparison with the MK-40 one. Hence, the factor of higher hydrophobicity of the MK-40 membrane seems determinative also.

When comparing MK-40 and MK-40′ membranes, let us calculate the local limiting current density, j_{lim}^{loc}, with respect to the area of conducting regions. It may be evaluated as $j_{lim}^{loc} = j_{lim}^{exp}/f_{cond}$, where j_{lim}^{exp} is the experimental limiting current density with respect to the total membrane area, f_{cond} (0.22 ± 0.03 for MK-40 and 0.30 ± 0.05 for MK-40′) is the surface fraction of ion-conducting particles. We have found that j_{lim}^{loc} in the cases of MK-40 (Fig. 6a) and MK-40′ (Fig. 6b) membranes is equal to 9.0 and 10.0 mA cm^{-2}, respectively, while the experimental values of the average limiting current density is 2.0 and 3.0 mA cm^{-2}, respectively. Thus the local limiting current through conducting regions of MK-40 and MK-40′ membranes is several times higher than the corresponding average experimental value and that calculated for homogeneous surface using the convection-diffusion model [40]. The corresponding theoretical values are close to those average experimental, 2.0 mA cm^{-2} and 2.5 mA cm^{-2}, respectively; they differ because the experimental conditions were different (Section 3).

Note that the local limiting current densities are rather close for both membranes while the values of f_{cond} are different. There are several reasons for high local limiting current density. The first one is the tangential transport of salt counterions from the solution situating near the non-conducting regions to the conducting ones: the electric current lines form a funnel-like pattern [45,47] (Fig. 7). The second one is the electroconvection, which is hastened by electrical inhomogeneity of the surface: the more significant heterogeneity yields greater the curl of the volume force.

The effect of hydrophobicity on electroconvection may be explained by repulsion between water molecules and a hydrophobic surface that causes slip of fluid over the surface [48,49]. Usually, the no-slip condition for the velocity is used: the fluid has zero velocity relative to the solid surface ($x = 0$):

$$V_x\big|_{x=0} = V_y\big|_{x=0} = 0. \tag{3}$$

This condition is supported by macroscopic experiments, in particular, in electrochemistry when non-intensive current regimes are applied [40]. Eq. (3) supposes that the effect of the surface on the fluid flow does not depend of the surface properties. However, the impact of surface phenomena increases and the surface properties become important when characteristic dimensions and fluid volumes are reduced [50,51] or intensive current regimes are applied.

To take into account the slip of fluid over hydrophobic surface, Navier has suggested the boundary condition expressed in the form [51]:

$$u_{slip} = b(\partial V_y/\partial n)_{x=0} \tag{4}$$

which relates the fluid tangential velocity u_{slip} at the surface and the shear strain rate normal to the surface, $\partial V_y/\partial n$, via the slip-length b; the velocity of the surface is set to zero. $b = 0$ relates to the no-slip condition, u_{slip} increases with increasing b.
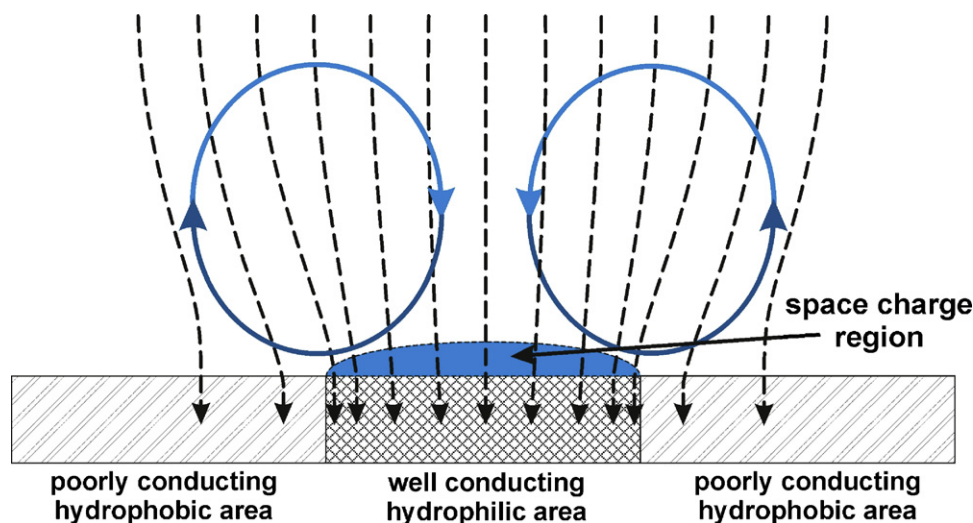
Fig. 7. A pair of electroconvective vortices formed near a depleted heterogeneous surface containing a well conducting and two poorly conducting areas; electric current lines are shown by dashed lines; schematic presentation.

Slip velocities on both hydrophilic and hydrophobic surfaces have been studied using a variety of experimental techniques [48,49,52,53]. The values of slip length reported vary from several nanometers [49] to as high as several tens of microns [53,54]. Majumder et al. [53] have found $b = 25\,\mu m$ from the pressure-driven flow rate measured through aligned multi-wall carbon nanotubes incorporated in a membrane. The flow velocity normalized at 1 bar was found to be $25\,cm\,s^{-1}$, that is 4 or 5 orders of magnitude faster than the evaluation by the Hagen–Poiseuille law. Hydrophobicity and, hence, the slip length can be significantly amplified by roughness [51].

In the case of ion-exchange membrane under high voltage, the maximum velocity of electroconvective vortex is approximately located at a distance from the membrane close to the position of the maximum of space charge density [26], that is of the order of hundred nanometers [14].

"The more hydrophobic surface, the higher overlimiting transfer rate" rule should be used with a care. Really, the hydrophobicity of the MK-40*/Nf is only slightly higher than that of the MK-40 membrane, however, the mass transfer rate is significantly larger in the case of MK-40*/Nf, being quite close to that of Nafion™ 117 (Figs. 6 and 10). This example shows the importance of the surface morphology, hence, the rule should work if the surface morphology of compared membranes is similar. We have mentioned that the most part (70–80%) of the MK-40 membrane is coated with polyethylene. On the one hand, this increases the contact angle on the surface, as polyethylene is a hydrophobic material and enhances electroconvection. But on the other hand, the local current density through conducting areas is about 3 times higher than the average current density, and that highly contributes to concentration polarisation of these regions and to the voltage across the membrane. In the case of MK-40*/Nf all the membrane surface is conductive, hence, the concentration polarisation (voltage) under the same average current density is lower. Moreover, the ion-exchange resin particles originated from MK-40 and risen over the surface (Fig. 4a) might make a considerable impact into decreasing contact angle, but a lower one into the reduction of electroconvection. Indeed, the material of resin particles having higher exchange capacity than Nafion is characterised also by higher specific conductivity. Hence, the local current density through these particles should be higher than the average current density. As a result, the extended SCR should be thicker, and the pressure produced by the volume force is higher near the resin particles than near neighbouring regions. This higher local pressure generates fluid motion from a resin particle towards the regions coated with Nafion material. This motion meeting inertial fluid layers produces paired vortices due to frictional interactions (Fig. 7). The main part of surface over which the vortex is slipping relates to more hydrophobic regions coated with Nafion. It can be seen from numerical calculations (Fig. 8) simulating the distribution of streamlines in a desalination channel where forced convection and electroconvection occur simultaneously. The simulation is made by solving the Navier–Stokes equations with no-slip boundary condition. The distribution of the electric volume force generating electroconvection was evaluated from a 1D model based on the Nernst–Planck and Poisson equations [39,55]. The maximum value of this force is approximately found as $f_{max} = (\rho E)_{max} \approx F c_{1s} E \approx \frac{RT}{D_1 F} j$ [55], where ρ is the electric charge density, E is the electric field strength, D_1 and c_{1s} are the diffusion coefficient and the minimum concentration of the counterion in the depleted diffusion layer. The force distribution is assumed to be trapezoidal. It is constant and equal to f_{max} within the space charge region of depleted solution near a conducting area of the surface, the thickness of the SCR is taken to be $10\,\mu m$. The force is zero near the non-conducting regions, and varies linearly in transitional zones. The morphology of the surface under modeling relates to a MK-40 cation-exchange membrane (Fig. 2). A conducting area includes an ion-exchange resin particle rising above the surface ($30\,\mu m$) and two transitional zones each of $1\,\mu m$ in length, which are spaces between the resin and the polyethylene filled with the bathing solution. The other part of the surface coated with polyethylene is non-conducting. The distance between the centers of conducting areas is $100\,\mu m$.

The vortices are approximately round, but not symmetrical due to the forced convection directed from left to right, and to the influence of the opposite membrane. The maximum of the vortex velocity relates to the transitional zones where the volume force varies and the curl of this force is not zero. As the vortices interact in the space between them (the zone of elevated pressure), they are also slightly shifted out of this space, towards the non-conducting areas associated in the case of MK-40 with the surface coated with polyethylene. The interior vortices are rather small, as their radius is limited by the half distance between the conducting areas. The external vortices are much greater, their size is limited by the opposite anion-exchange membrane. The forced flow fluid wraps around the vortices, which plays the role of obstacles for the forced flow.
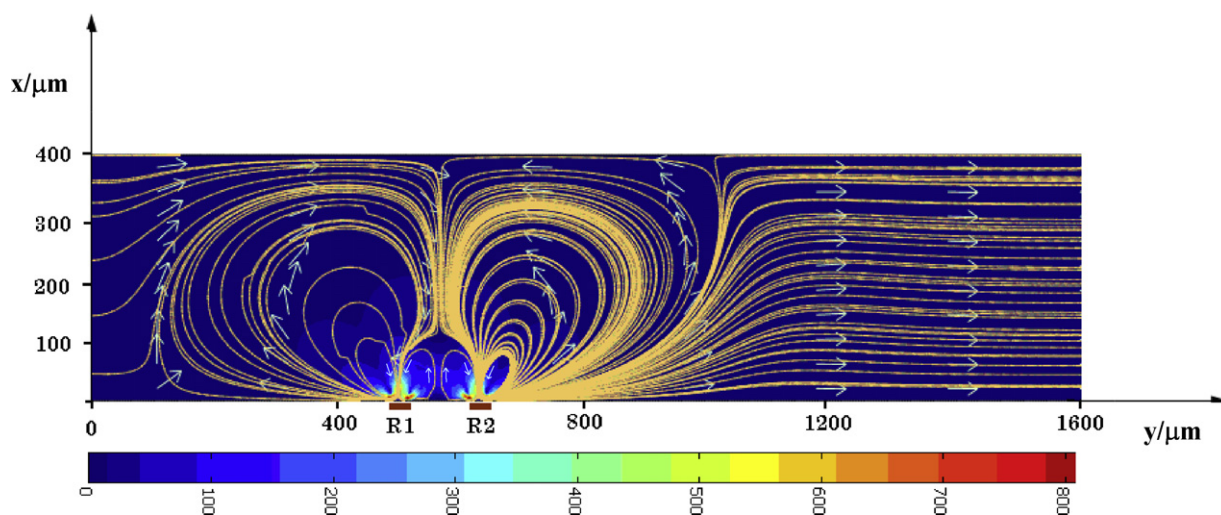
Fig. 8. Streamlines and velocity vectors of fluid flow in an electrodialysis desalination channel between two plane membranes; the channel height $H = 400\,\mu m$ and the length $L = 2200\,\mu m$ (a part of channel is shown); the maximum velocity of the forced flow $V_{max} = 0.5\,mm\,s^{-1}$, $Re = (V_{max}2h/\nu) = 0.4$. There are two conducting areas shown by rectangles R1 and R2. The volume force is normal to the surface; it is equal to f_{max} over the ion-exchange resin in the solution SCR decreases linearly to zero in the transitional zones. $f_{max} = 250\,N\,cm^{-3}$, that corresponds to the local current density $1\,mA\,cm^{-2}$.

To bypass the rightmost vortex, the forced flow passes between two biggest vortices, and then goes through a narrow "passage" near the right-hand side of the second conducting area R2. All the streamlines directed from left to right pass through this passage, whose thickness is close to the thickness of the SCR. Additionally, a part of the fluid transported by the rightmost vortex cycles and passes through the "passage" again. As a result, the volume rate of fluid flow through the "passage" is higher than the average flow rate in the channel, so that the tangential velocity here is much higher (more than 100 times) than the average forced flow velocity. Note that the simulation is rather qualitative as the thickness of the SCR $(10\,\mu m)$ is too high: an estimation made on the basis of the Nernst–Planck and Poisson equations has given $2\,\mu m$ for this magnitude in a cell of similar design where the voltage per cell pair was 8 V [14]. However, a decrease in the value of the SCR thickness leads to too high time of calculations.

Another parameter, which is different for the MK-40 and the MK-40*/Nf membranes is the dimension of "ion-conducting gates" for the electric current determined by the length between the extreme current lines entering the same conducting area [5]. For the MK-40, it is the diameter of a resin particle, that is about $30\,\mu m$. For the MK-40*/Nf, the "gate" is larger as there is a widening of current lines within the conducting Nafion film. As the size of a vortex is close to the diameter of the "gate" (which determines the width of the extended SCR), in the case of MK-40*/Nf the size of vortices should be higher, at least under relatively low voltages where the interaction between the vortices is weak.

3.5. MK-40-based membranes: mass transfer experiment

To obtain information about the behaviour of membranes under conditions close to real electrodialysis, we have measured the mass transfer coefficient in the ED cell shown in Fig. 1 as a function of inlet NaCl solution according to the method described in Section 3. The results obtained at $\Delta\varphi$ equal to 2 V across the membrane under study are shown as points in Fig. 9. The values of mass transfer coefficient are in a good accordance with the overlimiting currents presented in Fig. 3 and found for a $0.02\,mol\,dm^{-3}$ NaCl solution. The lowest mass transfer coefficient was observed in the case of the MK-40* membrane. The highest values of k were found for the MK-40*/Nf membrane.

It is important to note that the mass transfer coefficient increases, especially in the case of "good" membranes, with decreasing inlet NaCl solution. This behaviour may be explained by the fact that with diluting solution, the Debye length at the interface as well as the extended SCR thickness grow, under the same other conditions. The viscous forces hindering the development of electroconvection are less important at higher distance from the surface, hence, electroconvection becomes more intensive. However, in very diluted solutions, there is an opposite trend: k decreases with decreasing concentration. The cause is in water splitting at the membrane interface, which increases with decreasing solution concentration [4,30].
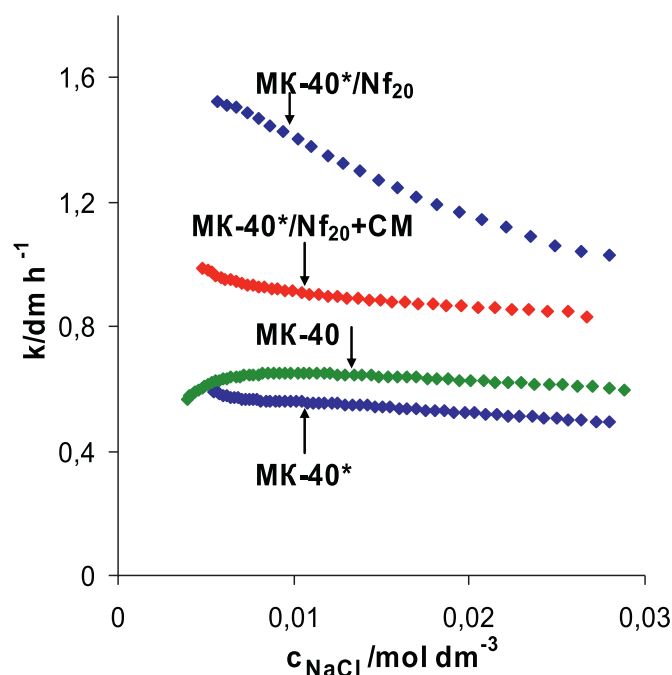

Fig. 9. Concentration dependence of the mass transfer coefficient of a MK-40 membrane and its modifications. The potential difference across the membrane under study is 2 V. The subscript number shows the thickness of Nafion surface layer in micrometers.

a

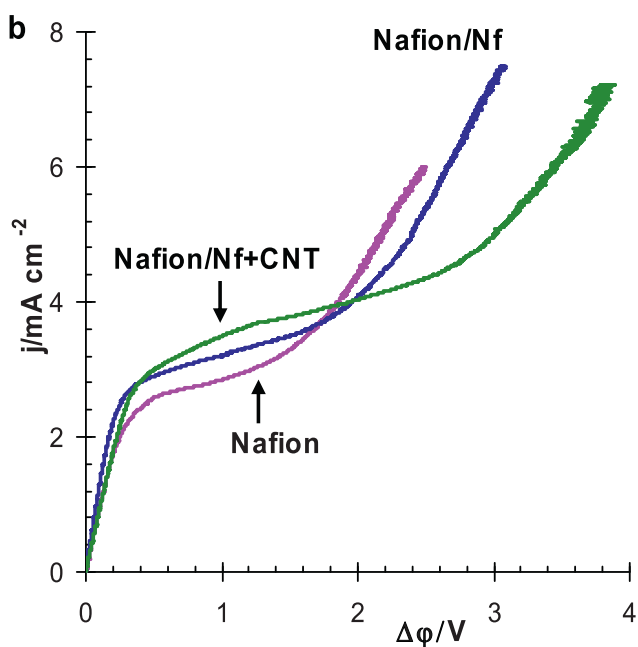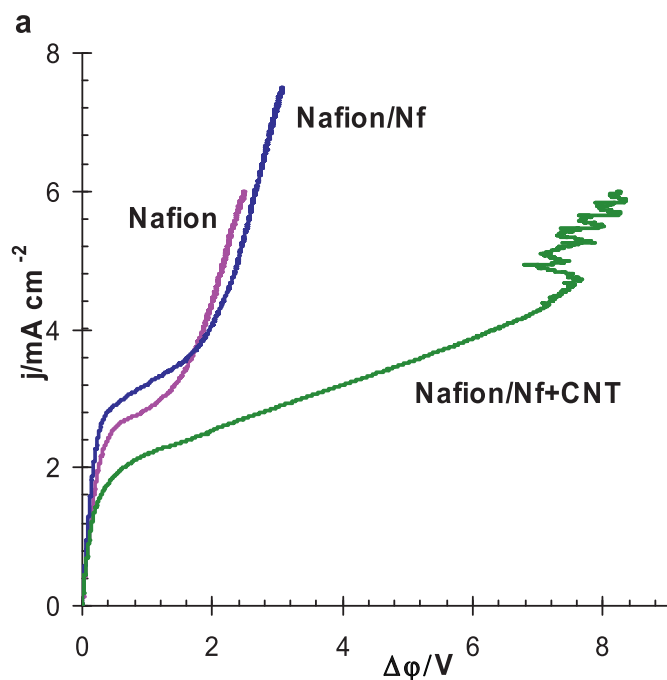Fig. 11. j_{lim}/j_{lim}^{theor} ratio as a function of the contact angle between water and the surface of ion-exchange membranes: MK-40 (1); MK-40′ (2); MK-40* (3); MK-40*/Nf (4); MK-40*/Nf + CM, (5); Nafion™ 117, unused and used (6); Nafion/Nf, unused (7); Nafion/Nf, used (8); Nafion/Nf + CNT, unused (9); Nafion/Nf + CNT, used (10). All the membranes prepared on the basis of MK-40 were studied "fresh", unused.

b

Fig. 10. Current–voltage characteristics of a commercial Nafion™ 117 membrane and its modifications: (a) "fresh" membranes not operated under electric current; (b) membranes after 100 h of operation under a current density $j = 1.5 j_{lim}$.

3.6. Nafion-based membranes

When preparing the MK-40*/Nf + CM membrane, we believed that addition of carbon material on the membrane surface will increase the surface hydrophobicity and, hence, the mass transfer rate. However, the effect was quite opposite: the degree of hydrophobicity was decreased, as well as the mass transfer rate. In order to better understand the obtained results, we have studied Nafion™ 117 membrane and two its modifications (Nafion/Nf and Nafion/Nf + CNT). Nafion™ 117 was used to exclude the factor of difference between the materials of the substrate and the film. Instead of carbon material, we have applied multiwall CNT. CNT, as
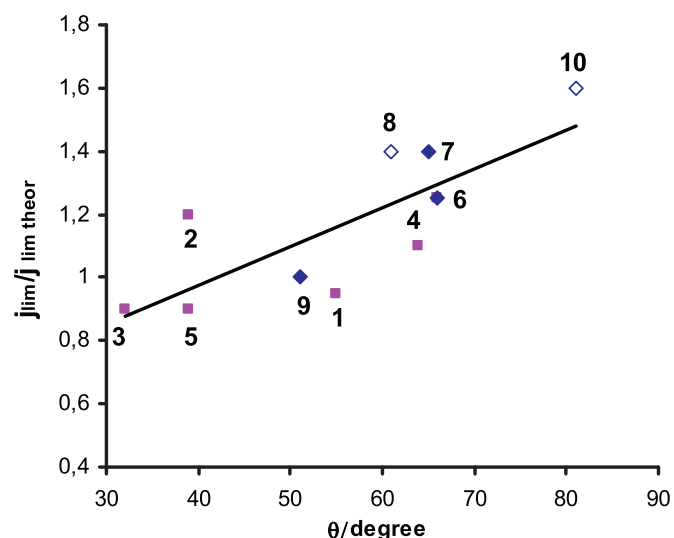
well as carbon material in the case of MK-40*/Nf + CM, forms conglomerates of the size of 1–10 μm covering about 15% of the surface (Fig. 5a). As it was noted above, the clusters of CNT are separated from the solution by a very thin "wall" of Nafion polymer of the thickness about 100 nm (Fig. 5c).

The effect of modification of Nafion membrane on the I–V characteristic is shown in Fig. 10a. The results are in agreement with those obtained for MK-40-based membranes. Coating a Nafion membrane with a Nafion film (Nafion/Nf) only slightly changes the I–V curve. The behaviour of both membranes is close to that of MK-40*/Nf while the limiting current density found by the intersection of the tangents drawn to the I–V curve at its beginning and at the "plateau" region is slightly higher in the case of the Nafion membrane. Note that this value, about 2.8 mA cm^{-2}, is significantly higher than the theoretical magnitude 2.0 mA cm^{-2}. The introduction of CNT into the Nafion film leads to a significant decrease in overlimiting transfer rate, similar as in the case of MK-40*/Nf + CM.

A rather unexpected result was the variation of the overlimiting transfer rate after operation of membranes under a relatively high current density equal to $1.5 j_{lim}^{theor}$ where $j_{lim}^{theor} = 2.0$ mA cm^{-2} as calculated by Eq. (1). The $\Delta\varphi$ across a membrane and two adjusting diffusion boundary layer was about 1.5 V. In the case of Nafion and Nafion/Nf samples, the variation in overlimiting transfer rate is negligible, remaining within the experimental error. However, in the case of Nafion/Nf + CNT sample, a significant increase of overlimiting mass transfer rate is observed. This rate is the highest among the studied membranes, in the range from 0.2 to 2 V.

Just after the coating, the Nafion membrane with a film containing CNT becomes more hydrophilic than the original membrane or a Nafion coated with a Nafion film not containing CNT (Table 2). Such behaviour, the same as in the case of MK-40*/Nf + CM, is explained by the formation of a wall of Nafion polymer enveloping the agglomerates of CNT (Fig. 5c) and reorientation of polymer chains within this wall. However, operation of Nafion/Nf + CNT under intensive current during 100 h leads to a strong increase in contact angle, from 51 to 81°. This is probably due to the partial destruction of the Nafion polymer wall, which separates the CNT agglomerates from the solution. The decrease in the thickness of the Nafion wall can be seen from the comparison of Fig. 5c and d. A significantly higher part of CNT is in fog (hence immersed deeper in the

film of Nafion) in the near-surface layer of the non-operated under current membrane in comparison with the operated membrane. As a result, the role of the Nafion wall decreasing effect of hydrophobicity of CNT on the surface comes down with the time of operation under current. This leads to an increase in surface hydrophobicity and, as a consequent, to an enhancement of overlimiting transfer.

The correlation of the limiting current density through all studied membranes, j_{lim} (found by the intersection of the tangents drawn to the beginning of the I–V curve and the plateau region, Figs. 6a, b and 10a, b) is shown in Fig. 11. It can be seen that the ratio of j_{lim} to the theoretical value of the limiting current density, j_{lim}^{theor}, found by Eq. (1) may be as high as 1.6. A similar correlation is found for overlimiting current density, if one fixes the same value of the potential drop for all membranes, in the range from 1 to 2 V.

4. Conclusions

Apparently, the main surface property affecting overlimiting mass transfer through an ion-exchange membrane is the degree of its hydrophobicity. The more the hydrophobic surface, the more readily water solution slips over this surface. This increased electroosmotic slip results in larger electroconvective vortices enhancing delivery of fresh solution from the bulk to the membrane surface. It is known that electrical inhomogeneity of surface facilitates electroconvection. However, coating an electrically inhomogeneous surface of a MK-40 membrane with a homogeneous hydrophobic Nafion film results in increasing overlimiting transfer. The effect is maximum in the case where carbon material or CNT are introduced into the Nafion film. But to attain this effect, a time of the order of 100 h of membrane operation in intensive current regime is needed. During this time, the surface hydrophobicity of the membrane is increasing, apparently, due to partial destruction of the Nafion polymer wall, which separates the clusters of carbon material from the solution.

Surface heterogeneity is also an important factor affecting electroconvection. The degree of hydrophobicity of the MK-40 membrane is only slightly lower than that of the MK-40*/Nf membrane, however, the overlimiting transfer across the latter is significantly higher than that across the former. The result is explained by the fact that too much of the MK-40 surface is coated with non-conducting polyethylene that causes high concentration polarisation of the conducting areas. Moreover, the contact angle is lower for the MK-40*/Nf membrane in comparison with Nafion™ 117 while the mass transfer rate is rather close for both membranes. The cause should be special surface morphology of the MK-40*/Nf membrane. Electrochemical behaviour of the coated with Nafion film heterogeneous MK-40 membrane tends to that of Nafion™ 117 when the thickness of the Nafion layer increases. The behaviour of both membranes becomes very close if thickness of the layer is about 20 μm.

Thus, by increasing surface hydrophobicity, it is possible to enhance overlimiting mass transfer through ion-exchange membranes, mainly controlled by electroconvection. In practical terms, this means that there are new opportunities to produce inexpensive ion-exchange membranes effective in electrodialysis of dilute solutions. This approach may be also interesting for other applications where the ability of this type of membranes to generate electrokinetic motion is used.

Acknowledgments

References

[1] I. Rubinstein, B. Zaltzman, O. Kedem, J. Membr. Sci. 17 (1997) 125.
[2] N.A. Mishchuk, Adv. Colloid Interface Sci. 160 (2010) 16.
[3] J. Balster, M.H. Yildirim, D.F. Stamatialis, R. Ibanez, R.G.H. Lammertink, V. Jordan, M. Wessling, J. Phys. Chem. B 111 (2007) 2152.
[4] E. Belova, G. Lopatkova, N. Pismenskaya, V. Nikonenko, C. Larchet, G. Pourcelly, J. Phys. Chem. B 110 (2006) 13458.
[5] V. Nikonenko, N. Pismenskaya, E. Belova, Ph. Sistat, Ch. Larchet, G. Pourcelly, Adv. Colloid Interface Sci. 160 (2010) 101.
[6] I. Rubinstein, B. Zaltzman, Phys. Rev. E 62 (2) (2000) 2238.
[7] S.S. Dukhin, Adv. Colloid Interface Sci. 35 (1991) 173.
[8] N.A. Mishchuk, S.S. Dukhin, in: A. Delgado (Ed.), Interfacial Electrokinetics and Electrophoresis, Marcel Dekker, New York, 2002, p. 241.
[9] M.Z. Bazant, T.M. Squires, Phys. Rev. Lett. 92 (6) (2004) 661011.
[10] B. Zaltzman, I. Rubinstein, J. Fluid Mech. 579 (2007) 173.
[11] S.S. Dukhin, N.A. Mishchuk, Colloid J. USSR 49 (1987) 1197.
[12] Z.M. Bazant, M.S. Kilic, B.D. Storey, A. Ajdari, Adv. Colloid Interface Sci. 152 (2009) 48.
[13] F.C. Leinweber, U. Tallarek, J. Phys. Chem. B 109 (2005) 21481.
[14] M.A.-K. Urtenov, E.V. Kirillova, N.M. Seidova, V.V. Nikonenko, J. Phys. Chem. B 111 (51) (2007) 14208.
[15] V.I. Zabolotskii, V.V. Nikonenko, Russ. J. Electrochem. 32 (2) (1996) 223.
[16] Y. Ben, E.A. Demekhin, H.-C. Chang, J. Colloid Interface Sci. 276 (2004) 483.
[17] V.M. Volgin, A.D. Davydov, Electrochim. Acta 49 (3) (2004) 365.
[18] R.B. Schoch, J. Han, Ph. Renaud, Rev. Modern Phys. 80 (2008) 839.
[19] J. Jong, R.G.H. Lammertink, M. Wessling, Lab. Chip 6 (2006) 1125.
[20] N.A. Mishchuk, T. Heldal, T. Volden, J. Auerswald, H. Knapp, Electrophoresis 30 (20) (2009) 3499.
[21] A. Ajdari, Phys. Rev. E 61 (2000) 45.
[22] D. Kim, J.D. Posner, J.G. Santiago, Sens. Actuators A 141 (2008) 201.
[23] N.A. Mishchuk, T. Heldal, T. Volden, J. Auerswald, H. Knapp, Microfluid. Nanofluid (2011), doi:10.1007/s10404-011-0833-2.
[24] A. Holtzel, U. Tallarek, J. Sep. Sci. 30 (2007) 1398.
[25] I. Rubinstein, B. Zaltzman, in: S. Sorensen (Ed.), Surface Chemistry and Electrochemistry of Membranes, Marcel Dekker, Basel/New York, 1999, p. 591.
[26] M.A.-K. Urtenov, Boundary Value Problems for Systems of the Nernst–Planck–Poisson Equations, Kuban State University, Krasnodar, 2000, p. 124 (in Russian).
[27] S.S. Dukhin, N.A. Mishchuk, Kolloidn. Zh. 51 (1989) 659 (in Russian).
[28] J.-H. Choi, H.-J. Lee, S.-H. Moon, J. Colloid Interface Sci. 238 (1) (2001) 188.
[29] N.D. Pismenskaya, V.V. Nikonenko, E.I. Belova, G.Yu. Lopatkova, P. Sistat, G. Pourcelly, C. Larchet, Russ. J. Electrochem. 43 (3) (2007) 307.
[30] R.A. Robinson, R.H. Stokes, Electrolyte Solutions, Butterworths, London, 1959.
[31] Y.J. Tanaka, J. Membr. Sci. 303 (2007) 234.
[32] J.J. Krol, M. Wessling, H. Strathmann, J. Membr. Sci. 162 (1–2) (1999) 145.
[33] R. Simons, Electrochim. Acta 29 (2) (1984) 151.
[34] V.I. Zabolotsky, N.V. Sheldeshov, N.P. Gnusin, Russ. Chem. Rev. 57 (8) (1988) 801.
[35] N.V. Gorachiy, Electromembrane Processes, Textbook, D. Mendeleyev University, Moscow, 2007 (in Russian).
[36] A.V. Nebavsky, K.A. Shevtsova, N.D. Pismenskaya, V.V. Nikonenko, Proceedings of the International Conference "Ion Transport in Organic and Inorganic Membranes", 2010, p. 121.
[37] M. Bass, A. Berman, A. Singh, O. Konovalov, V. Freger, J. Phys. Chem. B 114 (11) (2010) 3784.
[38] Sh. Goswami, Sh. Klaus, J. Benziger, Langmuir 24 (16) (2008) 8627.
[39] V.I. Zabolotsky, V.V. Nikonenko, Ion Transport in Membranes, Nauka, Moscow, 1996 (in Russian).
[40] J.S. Newman, Electrochemical Systems, Prentice Hall, Englewood Cliffs, N.J, 1973, p. 309.
[41] Pat. 100276 Russia, MPK51 G01N27/40 (2006.01) Device for the integrated study of mass transfer and electrochemical characteristics of ion-exchange membrane/N.D. Pismenskaya (Russia), V.V. Nikonenko (Russia), N.A. Melnik (Russia), E.I. Belova (Russia)-no. 2010129861/28; Appl. 07/16/2010; Publ. 10.12.2010.
[42] E.V. Lactionov, N.D. Pismenskaya, V.V. Nikonenko, V.I. Zabolotsky, Desalination 152 (2002) 101.
[43] N.D. Pismenskaya, E.I. Belova, V.V. Nikonenko, V.I. Zabolotsky, G.Yu. Lopatkova, Yu.N. Karzhavin, C. Larchet, Desalin. Water Treat. 21 (2010) 109.
[44] V.I. Zabolotsky, V.V. Nikonenko, N.D. Pismenskaya, J. Memb. Sci. 119 (1996) 171.
[45] E. Volodina, N. Pismenskaya, V. Nikonenko, C. Larchet, G. Pourcelly, J. Colloid Interface Sci. 285 (2005) 247.
[46] K.D. Kreuer, S. Paddison, E. Spohr, M. Schuster, Chem. Rev. 104 (2004) 4637.
[47] I. Rubinstein, B. Zaltzman, T. Pundik, Phys. Rev. E 65 (2002) 041507.

[48] N. Churaev, V. Sobolev, A. Somov, J. Colloid Interface Sci. 97 (1984) 574.
[49] C.-H. Choi, K.J.A. Westin, K.S. Breuer, Phys. Fluids 15 (10) (2003) 2897.
[50] T.M. Squires, S.R. Quake, Rev. Mod. Phys. 77 (3) (2005) 977.
[51] M.Z. Bazant, O.I. Vinogradova, J. Fluid Mech. 613 (2008) 125.
[52] R. Pit, H. Hervet, L. Leger, Phys. Rev. Lett. 85 (2000) 980.

[53] M. Majumder, N. Chopra, R. Andrews, B.J. Hinds, Nature 438 (2005) 44.
[54] O.I. Vinogradova, G.E. Yakubov, Langmuir 19 (2003) 1227.
[55] V.I. Zabolotsky, V.V. Nikonenko, N.D. Pismenskaya, M.Kh. Urtenov, E.V. Laktionov, H. Strathmann, M. Wessling, G.H. Koops, Sep. Purif. Technol. 14 (1998) 255.